Virchows Archiv (2019) 474:539–550
https://doi.org/10.1007/s00428-019-02533-9

ORIGINAL ARTICLE

β-Catenin nuclear expression discriminates deep penetrating nevi from other cutaneous melanocytic tumors

Arnaud de la Fouchardière[1,2] · Claire Caillot[1] · Julien Jacquemus[1] · Emeline Durieux[3] · Aurélie Houlier[1,2] · Véronique Haddad[1] · Daniel Pissaloux[1,2]

Received: 15 November 2018 / Revised: 21 January 2019 / Accepted: 25 January 2019 / Published online: 12 February 2019

Abstract

Recent advances in genomics have improved the molecular classification of cutaneous melanocytic tumors. Among them, deep penetrating nevi (DPN) and plexiform nevi have been linked to joint activation of the MAP kinase and dysregulation of the β-catenin pathways. Immunohistochemical studies have confirmed cytoplasmic and nuclear expression of β-catenin and its downstream effector cyclin D1 in these tumors. We assessed nuclear β-catenin immunohistochemical expression in a large group of DPN as well as in the four most frequent differential diagnoses of DPN: "blue" melanocytic tumors, Spitz tumors, nevoid and SSM melanomas, and pigmented epithelioid melanocytomas (PEM). Nuclear β-catenin expression was positive in 98/100 DPN and 2/16 of melanomas (one SSM and one nevoid melanoma with a plexiform clone) and was negative in all 30 Spitz, 26 blue, and 6 PEM lesions. In 41% DPN, β-catenin expression was positive in more than 30% nuclei. No differences were observed in cytoplasmic and nuclear cyclin D1 expression between these tumor groups, suggesting alternate, β-catenin-independent, activation pathways. We have subsequently studied nuclear β-catenin expression in a set of 13 tumors with an ambiguous diagnosis, for which DPN was part of the differential diagnosis. The three out of four patients showing canonical DPN mutation profiles were the only β-catenin-positive cases. We conclude that nuclear β-catenin expression, independently from CCND1 expression, in a dermal melanocytic tumor is an argument for its classification as DPN. In ambiguous cases and in early combined DPN lesions, this antibody can be helpful as a screening tool. β-Catenin is also potentially expressed in a subset of malignant melanomas with *CTNNB1* mutations.

Keywords Deep penetrating nevi · Beta catenin · Immunohistochemistry · Melanocytic tumors · Differential diagnosis

Virchows Archiv conforms to the ICMJE recommendation for qualification of authorship. The ICMJE recommends that authorship be based on the following four criteria:
- Substantial contributions to the conception or design of the work; or the acquisition, analysis, or interpretation of data for the work; AND
- Drafting the work or revising it critically for important intellectual content; AND
- Final approval of the version to be published; AND
- Agreement to be accountable for all aspects of the work in ensuring that questions related to the accuracy or integrity of any part of the work are appropriately investigated and resolved.

✉ Arnaud de la Fouchardière
arnaud.delafouchardiere@lyon.unicancer.fr

[1] Departement de Biopathologie, Centre Léon Bérard, 28, rue Laennec, 69008 Lyon, France

[2] Université Claude Bernard Lyon 1, INSERM 1052, CNRS 5286, Centre Léon Bérard, Cancer Research Center of Lyon, Equipe Labellisée Ligue contre le Cancer, Université de Lyon, Lyon, France

[3] Department of Pathology, Centre Hospitalier Lyon-Sud, 69310 Lyon, France

Introduction

Cutaneous melanocytic tumors are known for important variations of their morphologic appearance. In early lesions, distinction between several subtypes of nevi can be challenging. Atypical cases are often difficult to classify within any specific category. While genetic studies have enhanced the modern morpho-genetic classification, widely available techniques such as immunohistochemistry (IHC) can be a convenient first-line molecular tool in many pathology laboratories. Deep penetrating nevus (DPN) is a rare subtype of cutaneous melanocytic tumors that is often not recognized clinically [1]. DPN appears as small, dome-shaped, pigmented nodule(s) mainly located in the upper body region. It occurs in young adults with a slight female predominance. Histologically, its architecture can vary greatly [2]. The junctional component is inconstant and limited to scarce nests or lentiginous melanocytes without any pagetoid spread. The tumor is predominantly located in the dermis, forming a wedge-shaped silhouette at

scanning magnification [3]. Large spindled or epithelioid melanocytes with a wide cytoplasm often harboring thin melanin pigment are arranged in small nests or ill-defined fascicles. The nucleus is often large, oval, with prominent nucleoli. This peculiar cytology is found throughout the lesion without any maturation. The "DPN" denomination is related to vertically oriented expansions, usually following skin appendages, nerves, or blood vessels. Areas of spitzoid cytology with an eosinophilic cytoplasm can be identified. Mild lymphocytic infiltrates and intermingled melanophages are common features. Dermal fibrosis is limited, with patches of normal dermis often found in between nests. Superficial plexiform spindle cell nevus described by Barnhill et al. is the subject of an ongoing debate regarding its relationship with DPN [4, 5]. Combined DPN is a frequent variant of DPN in which a compound nevus with common cytology is associated with various amounts of pigmented nests with DPN cytology. When the disposition of the pigmented component is asymmetric, these combined DPN are often clinically worrisome and sent for referral as putative melanoma. Scolyer et al. have thoroughly discussed the pathogeny of combined nevi and favor the divergent terminal differentiation hypothesis based on the frequency of overlapping cytological features in merging areas [6]. DPN is frequently regarded as a difficult diagnosis as there are many similarities with plexiform and pigmented Spitz tumors, blue nevi, and pigmented epithelioid melanocytomas (PEM). In a recent study, we have shown that DPN are genetically defined by activation of both MAP kinase and β-catenin pathways [7]. This can occur through several combinations of events, the most frequent being combined *BRAF V600E* and exon 3 *CTNNB1* mutations. In that setting, strong nuclear β-catenin expression was present in the dermal DPN nests even when deeply located. DPN often arise from a pre-existing common acquired nevus resulting in a biphenotypic tumor where *CTNNB1* mutation is limited to the DPN component whereas the MAP kinase activating alteration is found in both components.

In this study, we compared β-catenin IHC expression profiles in an expanded panel of DPN and melanocytic lesions that are usual differential diagnoses of DPN: Spitz tumors, "blue" type tumors, PEM, and melanomas. A group of tumors with ambiguous morphological diagnosis was subsequently assessed. In a large subset of all these cases, cyclin D1 IHC expression and specific genetic drivers were also assessed.

Material and methods

Case selection

The cases were derived from the author's (AF) consultation cases (Centre Léon Bérard, Lyon, France). Archived slides with hematoxylin, eosin, and phloxin stain or IHC were checked for notable morphological and IHC features. The histological features in each selected sample were typical for each subtype of tumor. DPN were classified as either pure or combined when a common compound nevus component was associated. Cases were classified as atypical DPN according to the WHO classification when they had "atypical features such as large size, asymmetry, aberrant architecture (e.g. sheet-like arrangements of melanocytes), increased mitotic rates, and severe cytological atypia" [8]. Malignant variants of DPN, that would include the combination of all criteria, were excluded. "Blue" melanocytic tumors encompassed either common, or cellular, or sclerosing cellular blue nevus, or malignant blue melanoma ex-blue nevus. Spitz tumors were classified as either Spitz nevus or atypical Spitz tumor. Malignant Spitz tumors were excluded. PEM were of pure type. Melanomas were classified as either superficial spreading, or nodular, or nevoid melanoma according to the current WHO classification [8]. Neither acral lentiginous nor lentigo maligna melanoma was included. "Tumors with an ambiguous morphological diagnosis of DPN" were selected when nests of dermal pigmented epithelioid melanocytes suggested a potential diagnosis of DPN without all the usual morphological features including atypia or potential malignancy. Clinical information regarding gender, age at diagnosis, and topography of each lesion was obtained from the referring pathologist or the clinician. All cases were discussed in a multihead session including at least two senior dermatopathologists. The study was conducted according to the Declaration of Helsinki and has been approved by the Centre Léon Bérard's research ethics committee (Ref: L15-152). Sixty-eight DPN cases had been previously published [7].

Immunohistochemistry

Immunohistochemical staining was performed on 4 μm sections cut from formalin-fixed, paraffin-embedded (FFPE) tissue using a Ventana BenchMark Ultra automated stainer (Ventana, Tucson, USA) and revealed with the Enhanced Alkaline Phosphatase Red Detection Kit (Ventana #800-031). The following antibodies were used: β-catenin (clone beta catenin-1, 1:200, Dako), CCND1 (clone SP4, 1:1, Thermo Scientific), ALK (clone 5A4, 1:50, Novocastra), ROS1 (clone D4D6, 1:50, Cell Signaling), NTRK1 (clone EP1058Y, 1:200, Abcam), BRAF (clone VE1, 1:200, Spring Biosciences), BAP1 (clone C4, 1:50, Santa Cruz Biotechnology), p16 (clone E6H4, ready for use, Ventana), and PRKAR1A (rabbit polyclonal ab NB-22-20,039, 1:200, Neobiotech).

β-Catenin IHC expression was scored in dermal melanocytes (excluding subepidermal nests located immediately underneath the junction) according to the proportion of stained nuclei: score 0, 0%; score 1, < 10%; score 2, 10–30%; and

score 3, > 30% stained nuclei, regardless of any membranous and/or cytoplasmic staining (Fig. 1).

FISH technique

FISH was performed on 4 μm FFPE tissue sections, using the ZytoLight FISH-Tissue Implementation Kit (Zytovision # Z-2028-20, Bremerhaven, Germany) and a *PRKCA* break-apart probe (Empire Genomics # PRKCABA-20-ORGR, Buffalo, NY, USA), or a *CDKN2A* dual color probe (Zytovision # Z-2063-200), as per manufacturer's instructions. FISH signals were counted in at least 100 non-overlapping intact nuclei. A specimen was considered *PRKCA* positive if more than 20% of nuclei demonstrated a signal pattern consistent with a rearrangement (split of orange and green or single green without any corresponding orange signal). *CDKN2A* was considered heterozygously deleted if the percentage of nuclei showing only one green signal was above 50%.

G-proteins mutation study

Sequencing of exons 4 and 5 of *GNAQ* and *GNA11* or exon 3 of *CTNNB1* was performed as previously described [7, 9].

NGS sequencing

DNA was extracted from FFPE tissue sections using a Maxwell® 16 FFPE Plus LEV DNA Purification Kit (Promega). DNA was quantified by Qubit (Thermo Fisher Scientific, Cheshire, UK).

For each sample, 50 ng of DNA was used to prepare library with Solid Tumor Solution (Sophia Genetics, Saint Sulpice, Switzerland). Sequencing was performed (150 cycles paired end) with Miniseq High Output (Illumina).

The samples (minimum 1000× at each genomic position) were analyzed using Sophia DDM®.

RNA-seq

The total RNA was extracted from FFPE tissue sections using a Formapure RNA protocol (Beckman and Coulter). RNase-free DNase set (Qiagen, Courtaboeuf, France) was used to remove DNA. RNA was quantified by NanoDrop (Thermo Fisher Scientific, Cheshire, UK) and quality was controlled by TapeStation (DV200 value cutoff > 13%) with Hs RNA Screen Tape (Agilent, Courtaboeuf, France).

For each sample, 100 ng of total RNA was used to prepare library with TruSeq RNA Access Library Prep Kit (Illumina, San Diego, USA). Twelve libraries were pooled at 4 nM with 1% PhiX as an internal control. Sequencing was performed (75 cycles paired end) with NextSeq 500/550 High Output V2 kit in NextSeq 500 (Illumina).

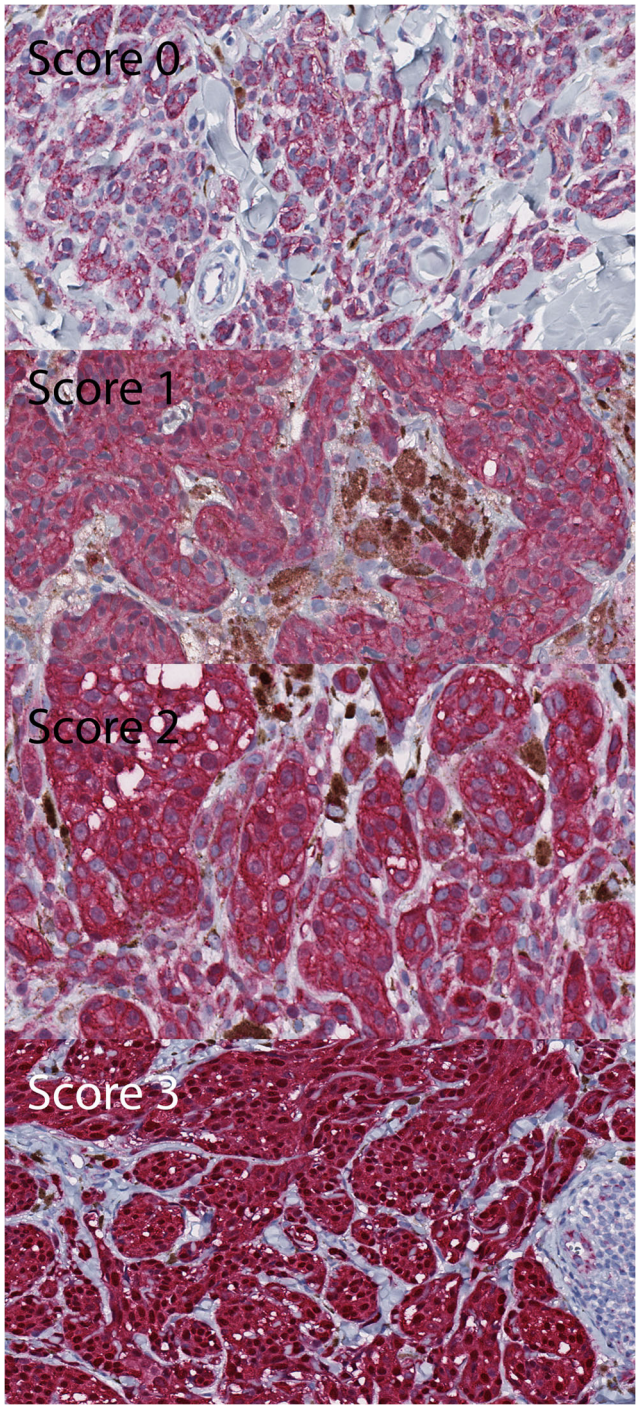

Fig. 1 Nuclear β-catenin IHC scoring. Score 0, weak cytoplasmic staining, no stained nuclei; Score 1, less than 10% of stained nuclei; score 2, between 10 and 30% of stained nuclei; score 3, more than 30% of stained nuclei

The samples (up to 80 million reads/sample) were analyzed. Alignments were performed with the STAR algorithm against the GRCh38 reference genome, and fusion gene assessments were made with STAR-Fusion, FusionCatcher, and FusionMap tools.

Results

Clinical, histological, immunohistochemical, and genetic features are summarized in Table 1.

DPN group

A total of 100 DPN were studied. Age at diagnosis ranged from 3 to 86 (median 39) years. There was slight female predominance (M/F ratio = 0.8). Lesions predominated in the upper body, with 60% located either on the head, upper limb, or trunk. Thirty-two percent were pure and 68% were combined DPN. β-Catenin nuclear expression was found in 98% cases. Scores 3, 2, and 1 were observed, respectively, in 41, 33, and 24% cases. Also, cytoplasmic and membranous expression of β-catenin was found in melanocytes regardless of nuclear staining (Fig. 2). Strong cytoplasmic and nuclear cyclin D1 expression was noted in all 82 tested cases. *BRAF* V600E mutation studied by IHC was present in 50% of the 76 tested cases and was more frequent in combined than in pure DPN (61.8 vs. 25%).

Spitz tumors group

Thirty cases were studied with 9 Spitz nevi and 21 atypical Spitz tumors. Age at diagnosis ranged from 2 to 53 (median 22.5) years. There was slight male predominance (M/F ratio = 1.14). Lesions predominated on the lower limb (53.5%). Nuclear β-catenin IHC was constantly found negative in dermal melanocytes (score 0, Fig. 3). Three of 30 cases had weak nuclear staining in superficial, subepidermal nests; a wild-type status of *CTNNB1* was tested and confirmed in one of these three cases. Also, cytoplasmic staining was constantly found with, in eight cases, granular distribution. Strong cytoplasmic and nuclear cyclin D1 expression was present in all 12 tested cases. High cytoplasmic protein expression levels of tyrosine kinases were identified by IHC in 21 cases (9 involving ALK, 8 involving NTRK1, and 4 involving ROS1).

"Blue" melanocytic tumors group

Twenty-six cases were studied: 2 melanomas ex-blue nevus, 20 cellular blue nevi (including 2 sclerosing subtypes), and 4 common blue nevi. Age ranged at diagnosis from 5 to 87 (median 37) years. There was no gender predominance (M/F ratio = 1).

Table 1 Main clinical, morphological, immunohistochemical, and genetic features

	DPN	Spitzoid group	Blue group	Melanoma	PEM
n	100	30	26	16	6
Age min–max (years)	3–86	2–53	5–87	20–81	3–37
M/F	0.8	1.14	1	2	0.5
Head	18	2	6	1	2
Trunk	37	1	1	8	1
Upper limb	15	9	2	4	2
Lower limb	29	16	13	1	0
Genital	0	1	2	0	1
Unknown	1	1	0	2	0
Benign	85	9	24	0	0
Atypical	15	21	0	0	6
Malignant	0	0	2	16	0
Bcat score 0 (%)	2	100	100	87.5	100
Bcat score 1 (%)	24	0	0	0	0
Bcat score 2 (%)	33	0	0	12.5	0
Bcat score 3 (%)	41	0	0	0	0
BRAF VE1 IHC	50/76	nd	nd	4/5	nd
CCND1 IHC	82/82	12/12	11/11	8/8	1/1
ALK IHC	nd	9/21	nd	nd	nd
NTRK1 IHC	nd	8/21	nd	nd	nd
ROS1 IHC	nd	4/21	nd	nd	nd
GNAQ/11 mutation (DNA sequencing)	nd	nd	6/7	nd	nd
PRKCA fusion (FISH)	nd	nd	nd	nd	2/2

nd not done

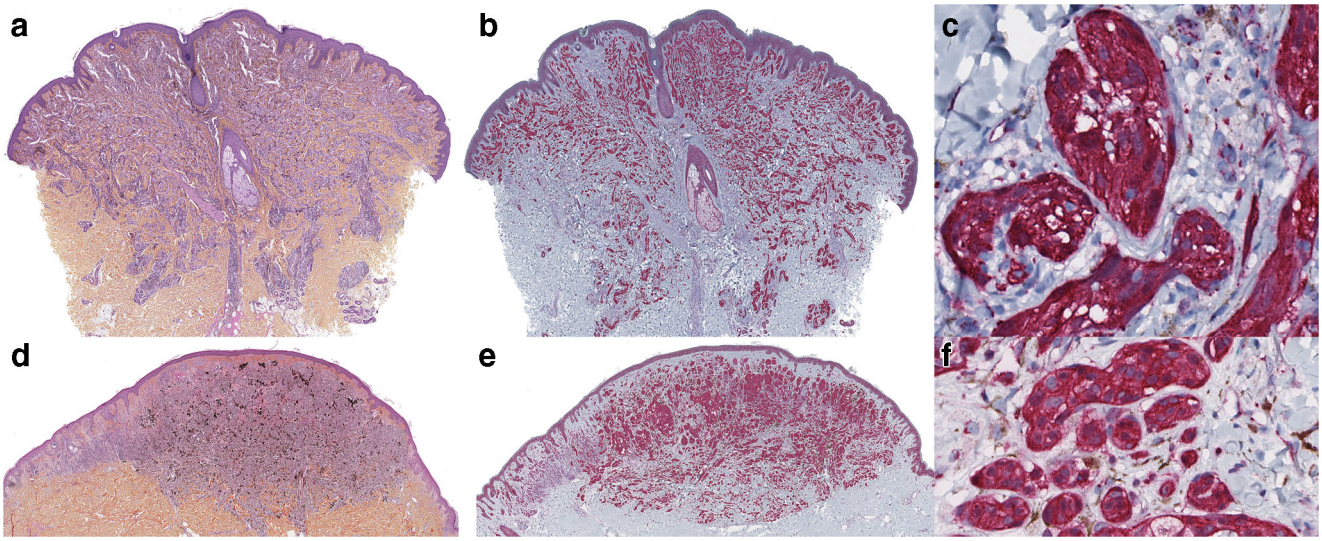

Fig. 2 DPN lesions: **a** pure DPN with deep expansions into the dermis [hematoxylin & eosin (H&E)]. **b** β-Catenin IHC with diffuse cytoplasmic staining. **c** β-Catenin IHC, close-up view, with nuclear staining (score 2) of vertical fasciculated strands of melanocytes. **d** Combined DPN with a lateral compound common nevus component on the left side and a pigmented DPN component with deep expansions into the dermis on the right side (H&E). **e** β-Catenin IHC showing diffuse positivity on the right side of the lesion and weak negative staining on the left side. **f** β-Catenin IHC, close-up view of the area where both component are present. Negative nuclear staining of the common melanocytes contrasting with cytoplasmic and nuclear staining of plexiform nests of melanocytes (score 2)

Fifty percent of cases were located on the buttocks/lower limb area. Nuclear β-catenin expression was absent (score 0) in all cases, including both malignant melanomas. Membranous and cytoplasmic staining was present both in benign and malignant cases (Fig. 4). Strong cytoplasmic and nuclear cyclin D1 expression was present in all 11 tested cases, with heterogeneous distribution in 4/11 cases. Protein G was mutated in 6/7 tested cases (5 *GNAQ* mutations and 1 *GNA11* mutation, all involving exon 5 canonical position Q209).

Primary cutaneous melanomas group

Sixteen cases were studied: 8 superficial spreading, 5 nevoid, and 3 nodular melanomas. Age at diagnosis ranged from 20 to 81 (median 48.5) years. Male predominance was present (M/F = 2.2). Lesions predominated on the trunk (50%) and upper limbs (25%). Breslow thickness ranged from 0.3 to 35 (median 2.1) mm. Nuclear β-catenin expression was rated as score 2 in 2/16 cases including one with a deep plexiform clone. In that case, nuclear positivity was restricted to the plexiform clone and negative in the surrounding nevoid melanocytes. The remaining 14/16 cases were negative (score 0), 4 of these showing membranous staining (Fig. 5). Granular cytoplasmic expression was found in one additional case. Cylin D1 expression was positive in all eight tested cases, with heterogeneous expression in six of them. *BRAF* V600E mutation was detected by IHC in 4/5 cases.

Pigmented epithelioid melanocytomas group

Six cases were studied. Age at diagnosis ranged from 3 to 37 (median 14.5) years. Female predominance was noted (M/F ratio = 0.5). No specific location was found. No nuclear β-catenin expression was found (score 0) in all 6/6 cases. Membranous and cytoplasmic staining was found in all 6/6 cases with variable intensity (Fig. 6). Cyclin D1 was positive in the only case that was assessed. A *PRKCA* rearrangement was identified in two cases by FISH.

"Tumors with an ambiguous morphological diagnosis of DPN" group

Thirteen cases were studied (Table 2). Age ranged from 5 to 73 (median 37) years. No specific location was found. Nuclear β-catenin expression, score 3, was found in 3/14 cases (Fig. 7). Subsequent molecular analysis confirmed combined *CTNNB1* and MAP kinase canonical mutations in these three cases but also in one β-catenin IHC-negative case. In the nine remaining cases, molecular studies showed a great variety of alterations. Canonical *CYSLTR2 p.L129Q* (two cases) or *GNAQ p.Q209L* mutations (one case) categorized lesions in the blue nevi group. One BAP1-inactivated melanocytic tumor was identified by nuclear BAP1 IHC loss. This case had a deep plexiform architecture and an important cytoplasmic pigmentation. Similarly, a case of PEM was diagnosed by a cytoplasmic PRKAR1A IHC expression loss. In two other cases, RNA sequencing found two undescribed in-frame gene

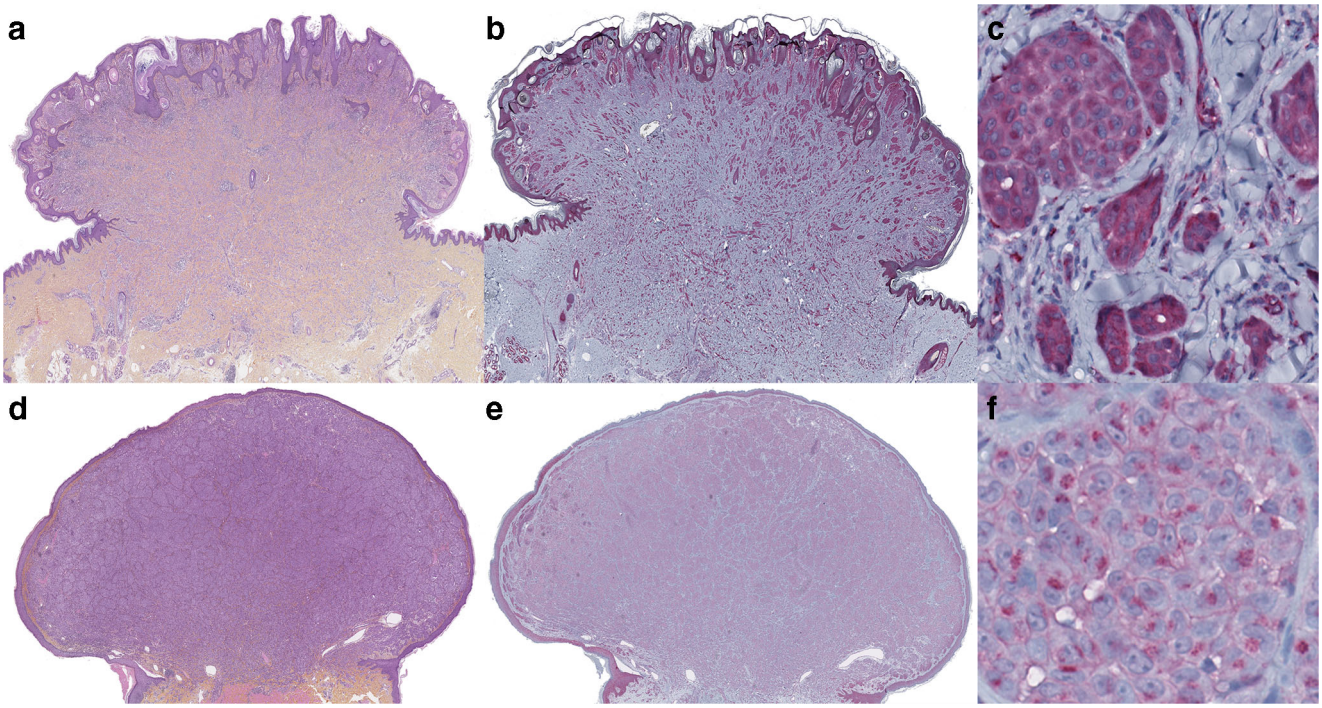

Fig. 3 Spitz tumors: **a** exophytic Spitz nevus with a dermal plexiform architecture associated with an *ALK* gene fusion [hematoxylin & eosin (H&E)]. **b** β-Catenin IHC: diffuse cytoplasmic staining underlining the plexiform architecture. **c** β-Catenin IHC close-up view showing no nuclear staining (score 0). **d** Exophytic atypical Spitz tumor with *NTRK1* gene fusion. **e** β-Catenin IHC weak diffuse positivity. **f** β-Catenin IHC close-up view showing no nuclear staining (score 0) and cytoplasmic dot-like clustering signal associated with a membrane positivity

fusions (*ATF7IP-USP32* or *ZNF555-DNAJA3*). The biological significance of such transcripts is currently unknown but no other known drivers were identified. At last, two cases with an initial combined/biphenotypic morphology associating a pigmented clone within a common compound nevus were potential DPNs. In one case, a *BRAF p.V600E* background was present and the atypical clone showed a loss of p16 confirmed as heterozygous by *CDKN2A* FISH. Regarding the importance of atypia, this clone was considered as malignant (nevoid melanoma ex-nevus). The second case had a *NRAS p.Q61R* background and showed a clone made of scattered melanocytes with a large heavily pigmented foamy cytoplasm. Mitotic figures were rare and proliferation index low. A final diagnosis of MelTUMP was made.

Discussion

In our previous study, we described alterations of both MAP kinase and β-catenin pathways as the genetic anomalies that define DPN [7]. Important variations of these genetic events were observed but the most frequent combination was association of both *BRAF p.V600E* and exon 3 *CTNNB1* canonical mutations. Another study had pointed out the presence of activating *HRAS* mutations in DPN [10]. We initially confirmed in 66/68 cases that membranous, cytoplasmic, and nuclear β-catenin immunoreactivity was strong in DPN while it showed top-heavy gradient in the adjacent common nevus in combined DPN [7]. In the current study, we focused on nuclear β-catenin IHC expression, as β-catenin accumulates in the cytoplasm but only has a transcriptional activity after being shuttled to the nucleus. Our results show that nuclear β-catenin IHC was positive in 98/100 DPN, hereby confirming our previous results [7]. Among these DPN, 41% were score 3. However, 24% were score 1 (< 10% stained nuclei), which indicates that special attention should be given when interpreting β-catenin IHC and high magnification screening might be necessary in some instances. In this group, the presence of a canonical *CTNNB1* mutation was assessed and present in 6/6 tested cases (data not shown) confirming that even with a low percentage of positive nuclei the β-catenin IHC is a valuable tool. β-Catenin IHC was able to easily detect only a few DPN nests in combined lesions, as well as DPN nests that were only slightly pigmented. The membrane and cytoplasm were constantly stained in all cases, even when nuclear score was 0. In combined DPN, which were more frequent than pure DPN, β-catenin IHC nuclear staining of the common nevus component was either negative or distributed with a "top-heavy" gradient. This eased microscopic interpretation: positive areas of DPN, even small nests, would stand out from the common nevus background. Interestingly, one of the IHC-negative DPN cases had two proven *CTNNB1 p.S45F* and *p.P52L* mutations and a *BRAF p.V600E* mutation (data not shown).

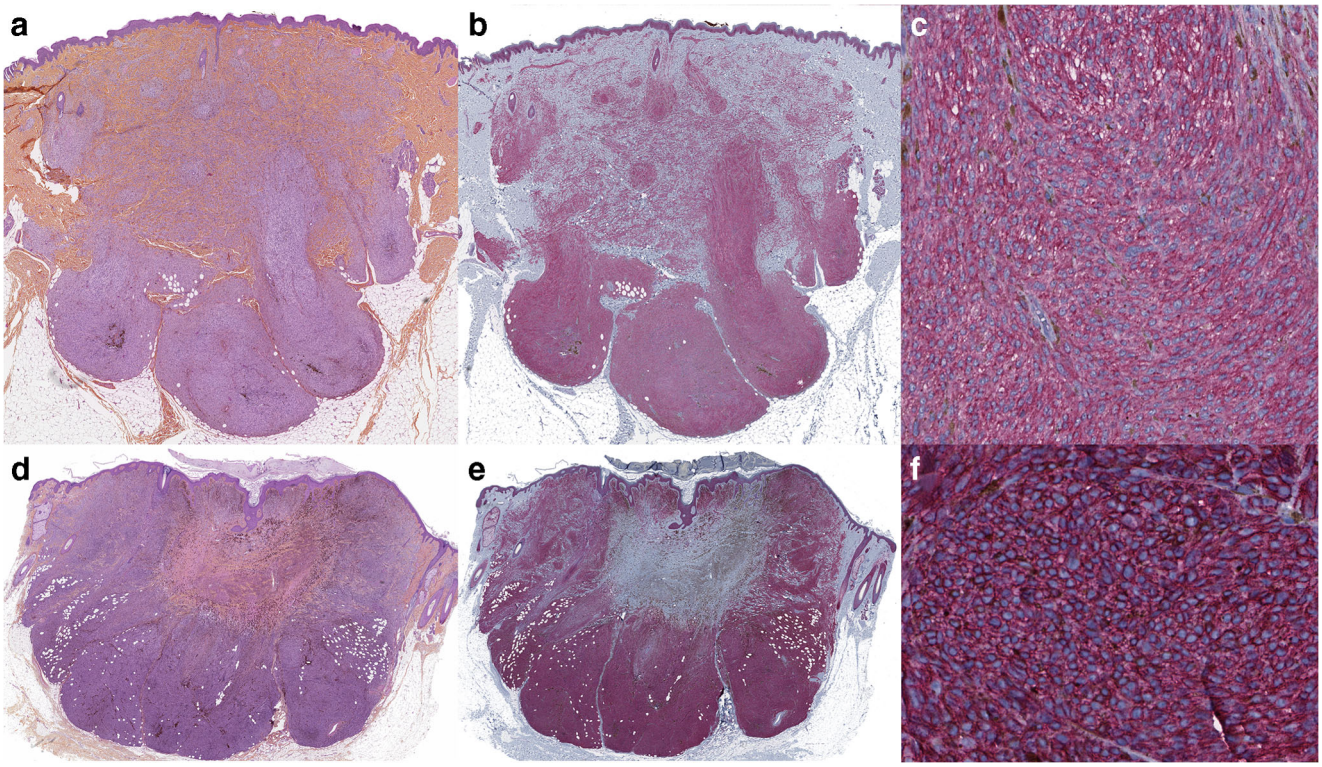

Fig. 4 Blue lesions: **a** cellular blue nevus with canonical biphasic architecture associating common blue nevus in the upper dermis and deep cellular expansions into the subcutis [hematoxylin & eosin (H&E)]. **b** β-Catenin IHC: diffuse cytoplasmic positivity. **c** β-Catenin IHC close-up view: positivity is restricted to the cytoplasm and membrane with blue unstained nuclei throughout the lesion (score 0). **d** Malignant blue melanoma ex-blue nevus with *GNA11 Q209L* mutation: dense dermal sheet of destructive melanocytes with focal hyperpigmented areas (H&E). **e** β-Catenin IHC: diffuse cytoplasmic staining. **f** β-Catenin IHC close-up view: positivity is restricted to the cytoplasm and membrane with blue unstained nuclei throughout the lesion (score 0)

This nearly constant positive nuclear β-catenin IHC staining pattern we herein described for DPN sharply contrasts with the lack of nuclear β-catenin expression in samples of main morphological differential diagnoses and adds to the delineation of DPN as a distinct entity among melanocytic tumors. Indeed, in many textbooks, including the former WHO classification, DPN was classified as a subgroup of blue nevus [11]. In recent studies, the driver mutations of blue nevi and related entities have been thoroughly explored with a predominance of protein G (exons 4 and 5 *GNAQ* and *GNA11* mutations) and less frequent *PLCB4* and *CYSLTR2* mutations [9, 12]. All of these events are mutually exclusive and clearly define blue tumors on the genetic level, but have not been observed in DPN. The differences in nuclear β-catenin IHC staining would further plead for classification of DPN as an entity unrelated to the blue nevi group. Spitz tumors also share overlapping dermal cytological features with DPN, especially in the architectural plexiform subtypes or in cases that are either weakly pigmented or with large dermal epithelioid cytology. In Spitz tumors, there is an expanding list of mutually exclusive genetic driver events that range from activating *HRAS* mutations to kinase fusions involving *ALK*, *ROS1*, *NTRK1*, *NTRK3*, *RET, BRAF,* and *MET* [13–16]. However, both *HRAS* mutations and *BRAF* kinase fusions have been described in DPN. We have intentionally selected Spitz cases without the latter anomalies to rule out any ambiguous diagnostic situation and to strengthen our initial results. The third group, PEM, may be difficult to distinguish from DPN not only because they can also arise as combined lesions from a *BRAF*-mutated nevus but also because of their heavily pigmented dermal epithelioid population. PEM are less frequent than blue or Spitz tumors. Initial cases have been associated with *PRKAR1A* mutations that are mostly somatic but can eventually be germline in the setting of Carney's complex [17, 18]. More recently, the genetics of PEM has been expanded with gene fusions involving *PRKCA* [19]. In our study, in all benign ($n = 33$) or intermediate ($n = 27$) differential diagnoses of DPN, nuclear β-catenin staining was negative outside the subepidermal area (score 0). Only slight subepidermal positivity was seen in 3/30 Spitz tumors, which suggests that these lesions could follow a distinct biology compared to the common nevi component of combined DPN in which this phenomenon is nearly constant. In the fourth differential diagnosis group composed of 16 primary cutaneous melanomas, we observed 2/16 nuclear β-catenin staining cases, both with score 2. In one of them, a deep pigmented subclone was present, as the upper part of the melanoma was stained negatively. These could represent

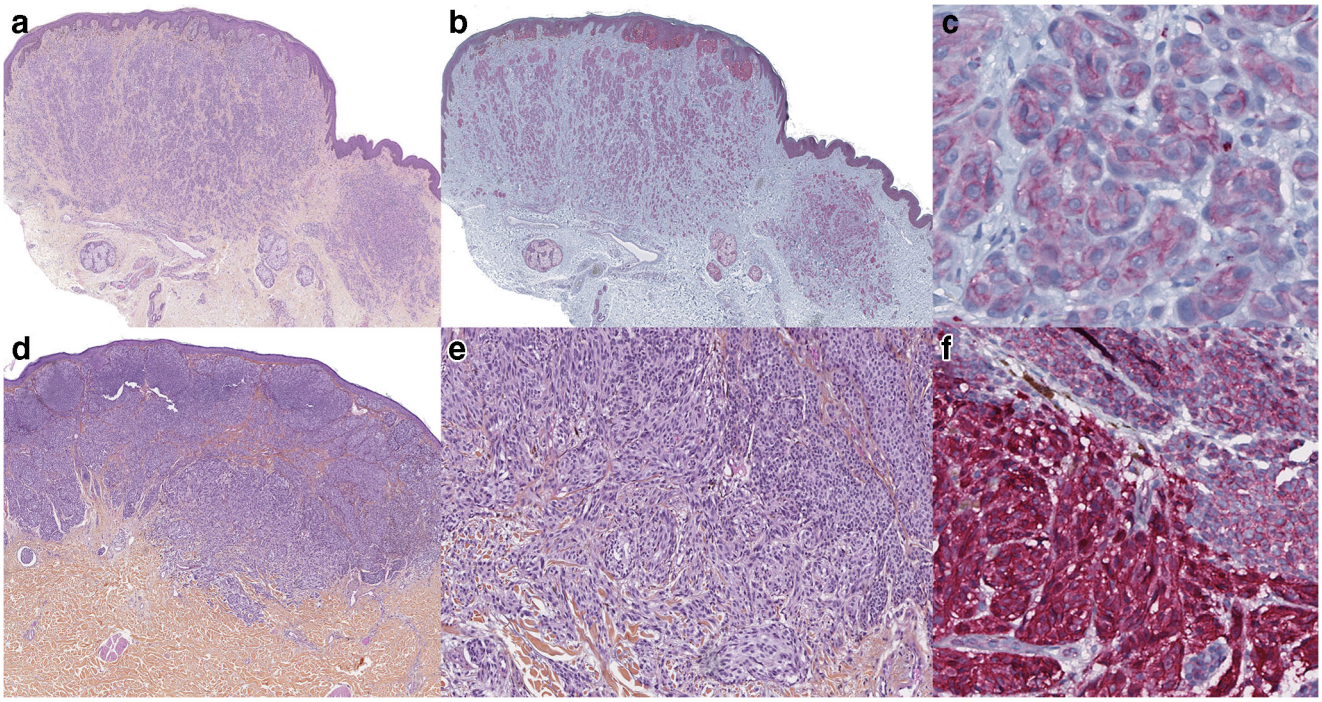

Fig. 5 Malignant melanomas: **a** low power view of nevoid melanoma, Clark level 4, Breslow 2.2 mm. The lesion is asymmetrical with dense dermal sheets of melanocytes devoid of maturation [hematoxylin & eosin (H&E)]. **b** β-Catenin IHC: diffuse weak cytoplasmic positivity. **c** β-Catenin IHC close-up view showing negative nuclear staining with weak cytoplasmic and membranous staining. (score 0). **d** Low power view of nevoid melanoma Clark level 4, Breslow 1.8 mm. The dermal component is made of dense sheets of destructive melanocytes (H&E). **e** Close-up view of a deep plexiform malignant clone with pigmentation (H&E). **f** β-Catenin IHC close-up view showing a strong cytoplasmic and nuclear signal in the plexiform clone (score 2) whereas the adjacent nevoid clone displays a weak cytoplasmic and membranous staining (score 0)

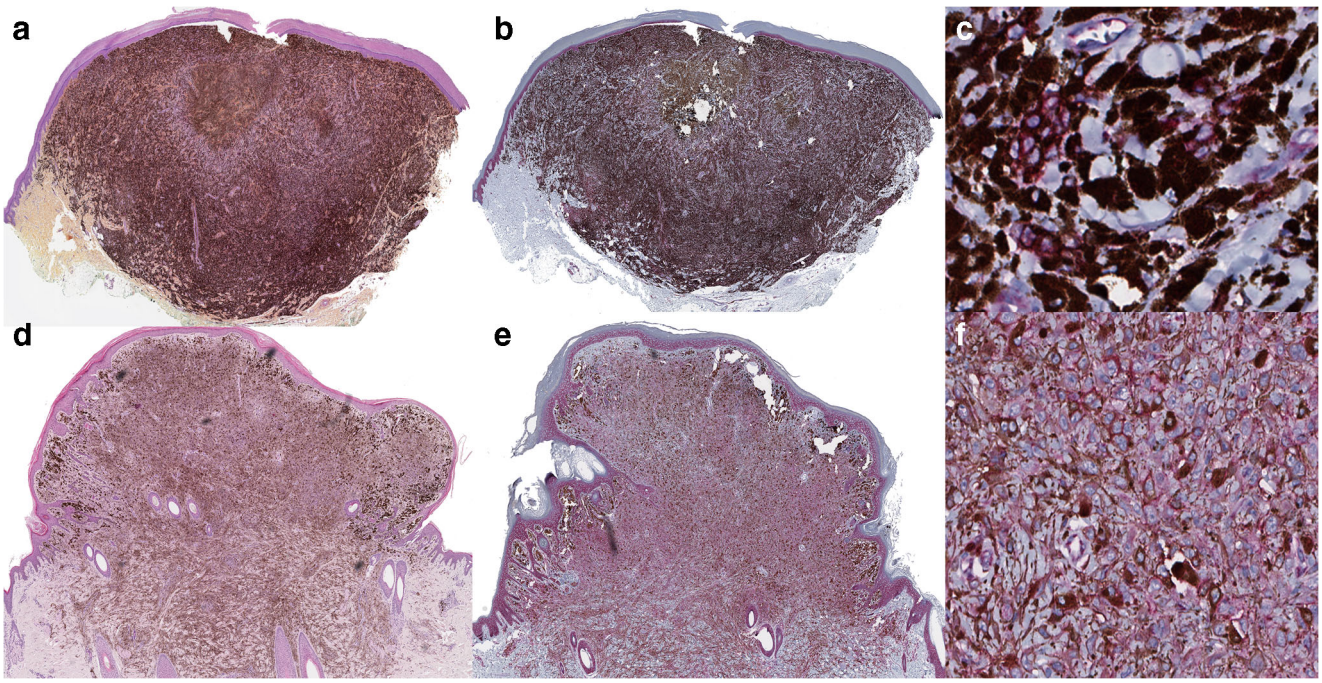

Fig. 6 : PEM lesions: **a** ill-limited, hyperpigmented proliferation with dispersed nests of melanocytes and a predominance of melanophages; focal necrotic area in the upper dermis [hematoxylin & eosin (H&E)]. **b** β-Catenin IHC with diffuse weak cytoplasmic positivity. **c** β-Catenin IHC close-up view with positive cytoplasmic and membrane staining and negative nuclear staining allowing the view of large central nucleoli (score 0). **d** Exophytic PEM with *PRKCA* fusion, the melanocytes are arranged in hyperpigmented sheets and fascicules expanding into the deep dermis with an ill-limited border H&E). **e** β-Catenin IHC with diffuse weak cytoplasmic positivity. **f** β-Catenin IHC close-up view with positive cytoplasmic and membrane staining and negative nuclear staining allowing the view of large central nucleoli (score 0)

Table 2 Clinical, morphological, and molecular data of confirmation cohort

	Sex/Age	Site	Initial diagnosis	CTNNB1 IHC score	Other genomic results	Final diagnosis
1	M/5	4	CBN vs DPN?	0	*GNAQ p.Q209L*	Compound CBN
2	F/10	2	Atypical DPN Vs SSM	0	*BRAF p.V600E* + *CTNNB1 p.S45F* array-CGH with no anomalies	Atypical DPN
3	F/24	4	DPN?	0	*ZNF555-DNAJA3* in frame fusion of unknown significance	MelTUMP
4	F/26	3	Atypical DPN?	3	*CTNNB1 p.S33F* + *MAP2K1 p.I103_K104del* + *ARID1A p.T1198A* Array-CGH : 9q loss	Atypical DPN
5	M/32	2	DPN vs PEM	0	PRKAR1A IHC loss	PEM
6	F/32	1	Combined DPN?	0	*BRAF p.V600E* + p16 IHC loss + FISH: heterozygous loss of CDKN2A	Nevoid melanoma
7	F/37	3	Combined DPN?	0	*NRAS p.Q61R* + *CDKN2A p.P114L*	MelTUMP
8	M/42	6	DPN vs PEM	0	*CYSLTR2 L129Q*	CBN
9	F/57	4	Unclassified dermal pigmented tumor	0	*CYSLTR2 L129Q*	Atypical CBN
10	M/62	2	Spitz nevus	3	*MAP2K1p.P105_A106del* + *CTNNB1 p.S33C*	Plexiform DPN
11	F/62	2	Unclassified dermal pigmented tumour	0	*BRAF p.V600E* + BAP1 IHC loss	BAP1-IMT
12	F/69	4	Malignant PEM vs DPN?	0	*ATF7IP-USP32* in frame fusion of unknown significance	Unclassified Melanoma
13	F/73	3	Unclassified dermal pigmented tumor	3	*BRAF p.V600E* + *CTNNB1 p.S45F*	DPN

Mutations are in red, gene fusions in purple, copy number variations in blue, and IHC expression loss in green

M male, *F* female, *site: 1* head and neck, *2* trunk, *3* upper limb, *4* lower limb including buttocks, *5* genital area, *6* unknown, *IHC* immunohistochemistry, *CBN* cellular blue nevus, *DPN* deep penetrating nevus, *PEM* pigmented epithelioid melanocytoma, *MelTUMP* melanocytic tumor of unknown prognosis, *BAP1-IMT* BAP1-inactivated melanocytic tumor, *CGH* comparative genomic hybridization, *FISH* fluorescent in situ hybridization

more aggressive melanoma and we suggest this should be studied in a larger group of lesions. Other morphologic features such as pagetoid scatter, grenz zone disappearance, and dermal density with mitotic activity should help identify the melanoma when β-catenin IHC is not discriminative. One must always stay alert as we have encountered the simultaneous occurrence of combined DPN and early SSM in several instances (data not shown).

Compared to β-catenin, cyclin D1 IHC was not discriminative, as it was found positive in all groups. This is possibly explained by multiple β-catenin-independent mechanisms (gene fusion, amplification) and/or activation pathways that can lead to cyclin D1 activation [20]. Previous IHC studies of cyclin D1 had focused on its weak expression in common nevi compared to melanomas [21–23]. This is the first study comparing DPN, Spitz, and blue subtypes of melanocytic

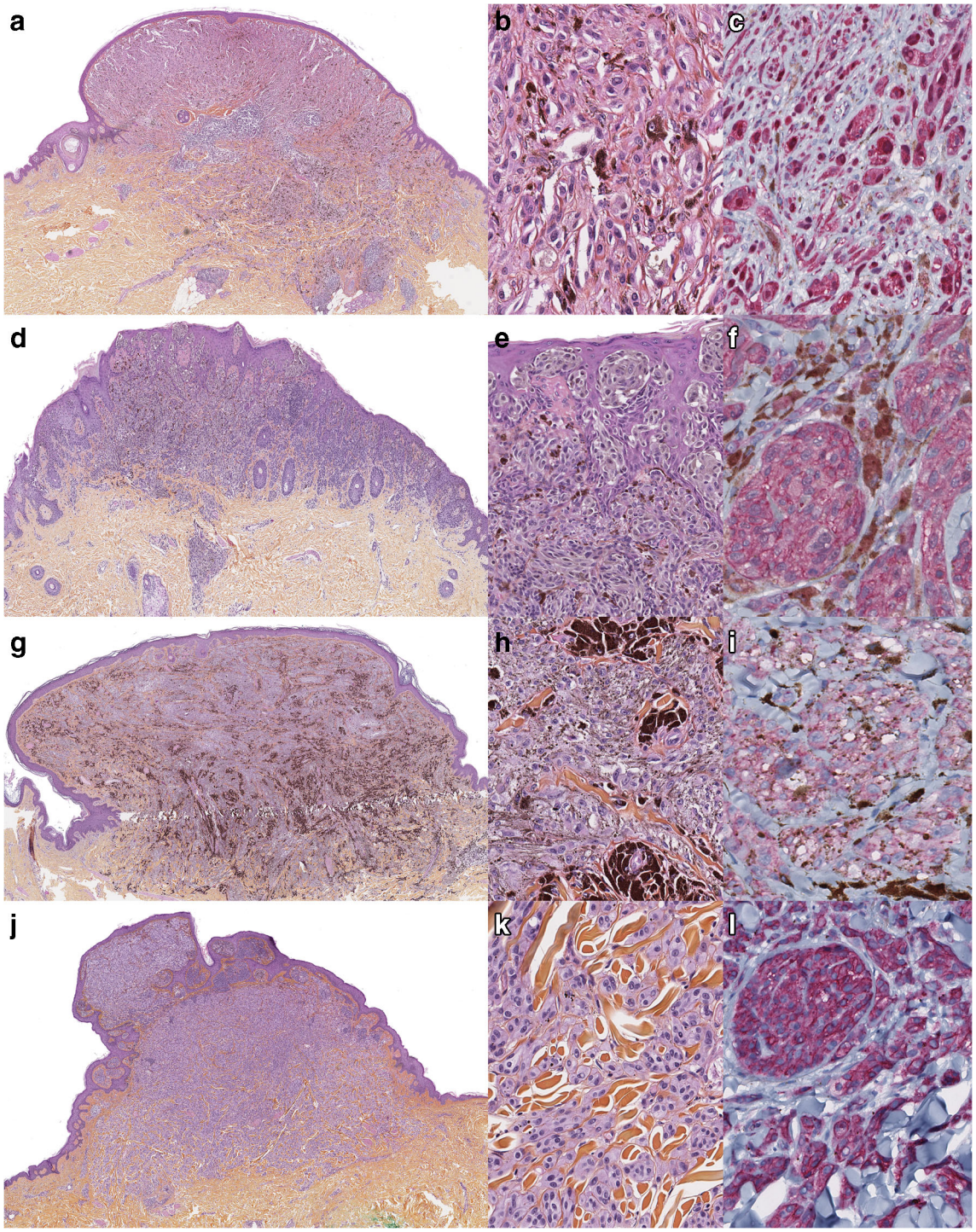

Fig. 7 Validation group: **a**, **b** atypical DPN (case 4) with dense superficial sheets of pleomorphic pigmented melanocytes. **c** β-Catenin IHC: strong cytoplasmic and nuclear staining. **d**, **e** Atypical DPN (case 2): dense dermal plexiform, pigmented and mitotic proliferation with superficial pagetoid spreading. **f** β-Catenin IHC: mild cytoplasmic staining without obvious nuclear positivity. **g**, **h** CBN (case 6) exophytic fasciculated proliferation of epithelioid and spindled hyperpigmented melanocytes with a fibrous background. **i** β-Catenin IHC: membranous staining with focal granular cytoplasmic positivity. **j**, **k** BAP1-inactivated melanocytic tumor (case 11) exophytic fasciculated dermal proliferation of epithelioid and spindled pigmented melanocytic without fibrosis. **l** β-Catenin IHC: strong cytoplasmic staining with bluish negative nuclei

tumors, underscoring a strong IHC staining intensity for cyclin D1 in all subgroups, and confirming weak staining intensity in common nevi.

BRAF p.V600E mutations in DPN were confirmed as a frequent event found in 50% of cases. This mutation-specific IHC can thus also be helpful to classify melanocytic lesions

within subgroups. If positive, it will rule out all conventional forms of Spitz tumors and blue melanocytic lesions. The background nevus in the combined variant of PEM, however, is also *BRAF p.V600E*-mutated and one would then have to rely more on morphological criteria and/or the loss of PRKAR1A IHC expression [19].

Following these results in well-documented groups, we assessed the reliability of β-catenin IHC in a more prospective manner, by using a validation set containing 13 tumors with an ambiguous morphological diagnosis of DPN, for which the final diagnosis was sought out, after performing β-catenin IHC, often by advanced molecular pathology techniques. The 3/13 cases that showed positive β-catenin nuclear staining also had *CTNNB1* and MAP kinase canonical mutations. One false negative case was seen confirming the IHC screening is not always reliable, just as it was only positive in 98% of the time in the initial study. There were, however, no false positive lesions. The great variety of final diagnoses included BAP1-inactivated nevus, blue tumors with unusual morphology, MelTUMP, nevoid melanoma, or PEMs reflects the difficulties of classifying pigmented dermal melanocytic tumors and the potential help positive β-catenin IHC screening can bring before more extensive molecular tests are performed.

In conclusion, this study shows that nuclear β-catenin IHC expression is a distinctive, and routinely accessible, feature that is both related to specific genetic events and helpful in distinguishing DPN from its most frequent differential diagnoses (blue or Spitz melanocytic tumors and PEM). Early SSM ex-nevi or nevoid melanomas remain potential pitfalls but have other distinctive morphological features. Cyclin D1 is expressed in all subtypes and cannot be relied on to classify these lesions.

Acknowledgments The authors thank the pathologists and dermatologist who contributed case material and clinical data as well as the patients for their participation in this study. The authors thank Elodie Legrand, Amandine Bernard, Cyrille Py, Sandrine Paindavoine, Florine Dreux, and Elise Malandain for their technical help as well as Iwei Yeh, Keisuke Goto, and Dr. Olivier Ramuz for their input on the manuscript. We thank Dr. Christiane Bailly and Dr. Christine Castillo for their participation in the diagnostic multihead sessions during the case selection process.

Contributions Arnaud de la Fouchardiere conceived and designed the study, and wrote, edited, and reviewed the manuscript. Julien Jacquemus, Emeline Durieux, and Aurélie Houlier researched and analyzed data. Claire Caillot, Véronique Haddad, and Daniel Pissaloux researched and analyzed data, and wrote, edited, and reviewed the manuscript. All authors gave final approval for publication. Author Arnaud de la Fouchardiere takes full responsibility for the work as a whole, including the study design, access to data, and the decision to submit and publish the manuscript.

Funding This work was funded by LYric grant INCa-DGOS-4664.

Compliance with ethical standards

The study was conducted according to the Declaration of Helsinki and has been approved by the Centre Léon Bérard's research ethics committee (Ref: L15-152).

Conflict of interest The authors declare that they have no conflict of interest.

References

1. Seab JA, Graham JH, Helwig EB (1989) Deep penetrating nevus. Am J Surg Pathol 13:39–44
2. Strazzula L, Senna MM, Yasuda M, Belazarian L (2014) The deep penetrating nevus. J Am Acad Dermatol 71:1234–1240. https://doi.org/10.1016/j.jaad.2014.07.026
3. Mehregan DA, Mehregan AH (1993) Deep penetrating nevus. Arch Dermatol 129:328–331
4. Barnhill RL, Mihm MC, Magro CM (1991) Plexiform spindle cell naevus: a distinctive variant of plexiform melanocytic naevus. Histopathology 18:243–247
5. Hung T, Yang A, Mihm MC, Barnhill RL (2014) The plexiform spindle cell nevus nevi and atypical variants: report of 128 cases. Hum Pathol 45:2369–2378. https://doi.org/10.1016/j.humpath.2014.08.009
6. Scolyer RA, Zhuang L, Palmer AA et al (2004) Combined naevus: a benign lesion frequently misdiagnosed both clinically and pathologically as melanoma. Pathology (Phila) 36:419–427. https://doi.org/10.1080/00313020412331283879
7. Yeh I, Lang UE, Durieux E, Tee MK, Jorapur A, Shain AH, Haddad V, Pissaloux D, Chen X, Cerroni L, Judson RL, LeBoit PE, McCalmont TH, Bastian BC, de la Fouchardière A (2017) Combined activation of MAP kinase pathway and β-catenin signaling cause deep penetrating nevi. Nat Commun 8:644. https://doi.org/10.1038/s41467-017-00758-3
8. Elder DE, Massi D, Scolyer R, Willemze R (eds) (2018) WHO classification of skin tumours. 4th ed. IARC Press, Lyon
9. Costa S, Byrne M, Pissaloux D, Haddad V, Paindavoine S, Thomas L, Aubin F, Lesimple T, Grange F, Bonniaud B, Mortier L, Mateus C, Dreno B, Balme B, Vergier B, de la Fouchardiere A (2016) Melanomas associated with blue nevi or mimicking cellular blue nevi: clinical, pathologic, and molecular study of 11 cases displaying a high frequency of GNA11 mutations, BAP1 expression loss, and a predilection for the scalp. Am J Surg Pathol 40:368–377. https://doi.org/10.1097/PAS.0000000000000568
10. Bender RP, McGinniss MJ, Esmay P et al (2013) Identification of HRAS mutations and absence of GNAQ or GNA11 mutations in deep penetrating nevi. Mod Pathol 26:1320–1328. https://doi.org/10.1038/modpathol.2013.77
11. LeBoit PE, Burg G, Weedon D, Sarasin A (eds) (2006) Pathology and genetics of skin tumours. IARC Press, Lyon
12. Griewank KG, Müller H, Jackett LA et al (2017) SF3B1 and BAP1 mutations in blue nevus-like melanoma. Mod Pathol 30:928–939. https://doi.org/10.1038/modpathol.2017.23
13. Bastian BC, LeBoit PE, Pinkel D (2000) Mutations and copy number increase of HRAS in Spitz nevi with distinctive histopathological features. Am J Pathol 157:967–972. https://doi.org/10.1016/S0002-9440(10)64609-3
14. Wiesner T, He J, Yelensky R, Esteve-Puig R, Botton T, Yeh I, Lipson D, Otto G, Brennan K, Murali R, Garrido M, Miller VA, Ross JS, Berger MF, Sparatta A, Palmedo G, Cerroni L, Busam KJ, Kutzner H, Cronin MT, Stephens PJ, Bastian BC (2014) Kinase fusions are frequent in Spitz tumours and spitzoid melanomas. Nat Commun 5:. https://doi.org/10.1038/ncomms4116
15. Yeh I, Botton T, Talevich E, Shain AH, Sparatta AJ, de la Fouchardiere A, Mully TW, North JP, Garrido MC, Gagnon A,

Vemula SS, McCalmont TH, LeBoit PE, Bastian BC (2015) Activating MET kinase rearrangements in melanoma and Spitz tumours. Nat Commun 6:7174. https://doi.org/10.1038/ncomms8174

16. Yeh I, Tee MK, Botton T, Shain AH, Sparatta AJ, Gagnon A, Vemula SS, Garrido MC, Nakamaru K, Isoyama T, McCalmont TH, LeBoit PE, Bastian BC (2016) NTRK3 kinase fusions in Spitz tumours. J Pathol 240:282–290. https://doi.org/10.1002/path.4775
17. Zembowicz A, Carney JA, Mihm MC (2004) Pigmented epithelioid melanocytoma: a low-grade melanocytic tumor with metastatic potential indistinguishable from animal-type melanoma and epithelioid blue nevus. Am J Surg Pathol 28:31–40
18. Mandal RV, Murali R, Lundquist KF, Ragsdale BD, Heenan P, McCarthy SW, Mihm MC, Scolyer RA, Zembowicz A (2009) Pigmented epithelioid melanocytoma: favorable outcome after 5-year follow-up. Am J Surg Pathol 33:1778–1782. https://doi.org/10.1097/PAS.0b013e3181b94f3c
19. Cohen JN, Joseph NM, North JP, Onodera C, Zembowicz A, LeBoit PE (2017) Genomic analysis of pigmented epithelioid melanocytomas reveals recurrent alterations in PRKAR1A and PRKCA genes. Am J Surg Pathol 41:1333–1346. https://doi.org/10.1097/PAS.0000000000000902
20. Sauter ER, Yeo U-C, von Stemm A, Zhu W, Litwin S, Tichansky DS, Pistritto G, Nesbit M, Pinkel D, Herlyn M, Bastian BC (2002) Cyclin D1 is a candidate oncogene in cutaneous melanoma. Cancer Res 62:3200–3206
21. Georgieva J, Sinha P, Schadendorf D (2001) Expression of cyclins and cyclin dependent kinases in human benign and malignant melanocytic lesions. J Clin Pathol 54:229–235
22. Ramirez JA, Guitart J, Rao MS, Diaz LK (2005) Cyclin D1 expression in melanocytic lesions of the skin. Ann Diagn Pathol 9:185–188. https://doi.org/10.1016/j.anndiagpath.2005.04.018
23. Alekseenko A, Wojas-Pelc A, Lis GJ, Furgał-Borzych A, Surówka G, Litwin JA (2010) Cyclin D1 and D3 expression in melanocytic skin lesions. Arch Dermatol Res 302:545–550. https://doi.org/10.1007/s00403-010-1054-3